SAE INTERNATIONAL

Determining Position and Speed through Pixel Tracking and 2D Coordinate Transformation in a 3D Environment

2016-01-1478
Published 04/05/2016

William T. Neale, David Hessel, and Daniel Koch
Kineticorp LLC

CITATION: Neale, W., Hessel, D., and Koch, D., "Determining Position and Speed through Pixel Tracking and 2D Coordinate Transformation in a 3D Environment," SAE Technical Paper 2016-01-1478, 2016, doi:10.4271/2016-01-1478.

Abstract

This paper presents a methodology for determining the position and speed of objects such as vehicles, pedestrians, or cyclists that are visible in video footage captured with only one camera. Objects are tracked in the video footage based on the change in pixels that represent the object moving. Commercially available programs such as PFTrack[tm] and Adobe After Effects[tm] contain automated pixel tracking features that record the position of the pixel, over time, two dimensionally using the video's resolution as a Cartesian coordinate system. The coordinate data of the pixel over time can then be transformed to three dimensional data by ray tracing the pixel coordinates onto three dimensional geometry of the same scene that is visible in the video footage background. This paper explains the automated process of first tracking pixels in the video footage, and then remapping the 2D coordinates onto three dimensional geometry using previously published projection mapping and photogrammetry techniques. The results of this process are then compared to VBOX recordings of the objects seen in the video to evaluate the accuracy of the method. Some beneficial aspects of this process include the time reduced in tracking the object, since it is automated, and also that the shape and size of the object being tracked does not need to be known since it is a pixel being tracked, rather than the geometry of the object itself.

Introduction

Camera matching photogrammetry is an established technique for determining where, in a scaled three dimensional environment, an object is located that is visually represented in a two dimensional photograph [1,2,3,4]. Though a photograph is only a two dimensional image, it visually represents a three dimensional world, and techniques of camera matching photogrammetry allow the position, orientation and scale of objects visible in the photograph to be located in a three dimensional environment through laws of perspective. The camera characteristics of the camera used to photograph a scene can be rectified through a reverse camera projection process [1,2,3,4]. When this camera is used to view the digital photograph against the background of a three dimensional computer environment that represents the same geometry as that seen in the photograph, objects that appear in the photograph, that are not present in the computer model, can be "matched" in the camera, and subsequently its location and orientation can also be matched in the computer environment. Video is a series of still images, captured at a rate that when played back, appears to show motion of objects. Since camera matching has been validated for a single image, it is also valid for a series of single images. In other words, camera matching an object in one image is the same process as camera matching the position of an object over several images, though the result of matching several images is that the change in position can also be determined. Previous literature has developed the technique of tracking video in this manner [5,6,7]. However, to track an object in a video using camera matching photogrammetry, the location of the object must be manually matched at each frame that is being analyzed, which can be time consuming. Additionally, for tracking objects through camera matching photogrammetry, the size and shape of the vehicle is often also needed, since the size and shape of the object is relied upon to get good position and orientation of the object. Coleman, et. al. [2] validate a technique of camera matching that utilizes three dimensional scan data to both assist in determining the camera characteristics of the photograph that took the image, as well as locating objects in the photograph that are no longer in the scene. In an effort to develop a technique that can help automate the process of tracking an object in video, this paper uses the same concepts of camera matching photogrammetry, (i.e. matching the camera characteristics in a scanned three dimensional scene). However, rather than tracking an object by matching its three dimensional position through multiple frames of the video, which can be time intensive, this paper examines the use of automated pixel tracking, and ray trace projection to automatically locate the object in three dimensional space.

Concept of 2D Coordinate Transformation

The tracking of objects in video, also called motion tracking, can be a manual or automated process where, in an x and y coordinate system determined by the video's resolution, a discrete pixel, or series of pixels are located at various frames. Figure 1 shows the coordinate grid of a standard high definition image, with lines at intervals of 64 pixels.

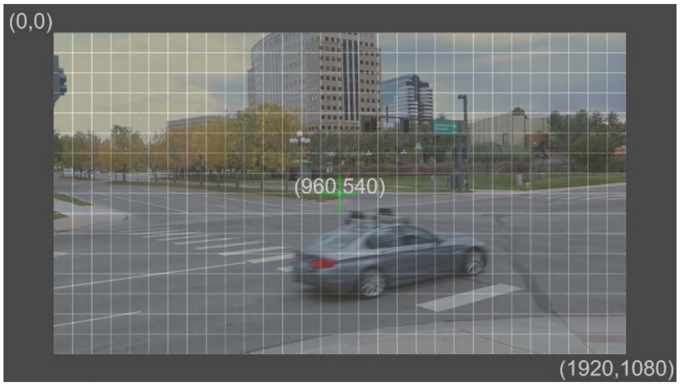

Figure 1. Coordinate grid for a video frame

The top left pixel would be considered 0,0, and the bottom right pixel 1920,1080. In this manner, each pixel has a unique location in the video frame. As the object moves in the video, the object will be represented by different pixels that occupy different position in the video frame over time. Figure 2 demonstrates this concept of an object moving across the video frame, and the tracking concept that continually determines the position of the pixels representing this object over time. The chart in Figure 3 is an example of the x and y coordinates that would be recorded from the pixel tracking process.

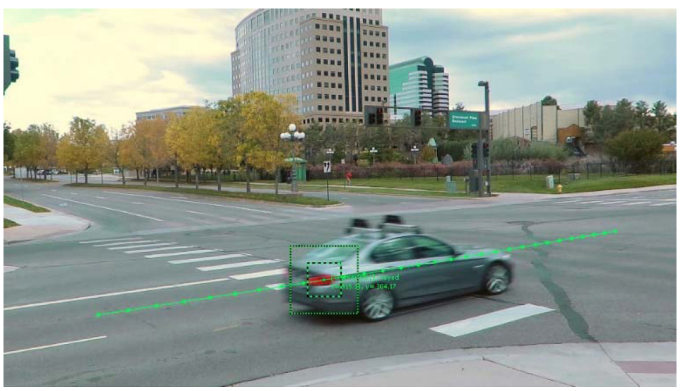

Figure 2. Concept of pixel tracking

Frame	X	Y
5254	-11.449	160.6268
5257	270.5601	204.5128
5258	356.3163	217.6151
5259	437.7351	230.4421
5260	515.7413	242.4254
5261	589.6788	253.7067
5262	661.1851	264.7584
5263	729.7164	275.4664
5264	794.6101	285.4557
5265	856.6101	294.8885

Figure 3. Matrix coordinates resulting from tracking a pixel

In this paper's research, automatic tracking of pixels in video was performed using PFTrack^{tm} and Adobe After Effects programs, though there are several other programs designed for this same specific purpose [8]. PFTrack^{tm} is one of several available professional match moving software applications. This software is designed primarily to track the movement of a camera through a video shot so that the same motion observed in the video shot can be duplicated but with a virtual camera. PFTrack^{tm} performs this analysis by tracking pixels of common characteristics, and using principles of photogrammetry and parallax to solve the location of the camera. Likewise, PFTrack^{tm} pixel tracking modules can be used to track pixel and determine the location of the pixel as it appears in the frame of the video. Because each pixel has a signature between 0 and 256 (for 8 bit images which includes most video) and each pixel is usually surrounded by other pixels with a different value, however subtle, a program can automatically track the location of the pixels that are representing an object in the video. Where the pixel changes its value or position dramatically, most programs allow checking and adjusting of its tracking to ensure its accuracy. Because the video image has a set resolution, the width and height of the image can be determined. These dimensions are in pixels, denoting length and width that the pixel is from the top left position of the image. As the tacking software determined the location of the pixel in the video image, its two dimensional coordinate can be determined as Cartesian x and y values.

Having tracked the position of a pixel in a video, and converted the coordinates to a matrix of x and y values, principles of camera matching photogrammetry are utilized to determine the positon of the camera in three dimensional space. [1,2,7]. This requires creating geometry, from scanning, surveying or other methods, of the scene represented in the video. Next PFTrack was used to solve for the location of the camera buy selecting known points visible in the video and assigning them a 3D point in the LIDAR scan data. In this process of camera matching, once at least 4 points have been assigned the software can automatically solve the 3D camera location and camera characteristics.

To transform the 2D coordinates from the tracking on to the three dimension geometry of the scene, ray tracing and projection mapping technology is used to essentially "fire" a point from the camera, at an angle laterally and vertically relative to the cameras orientation that is determined by the pixels coordinate. The firing of this ray through the determined angles transforms the two dimensional location into the three dimensional environment. Figure 4 is a graphical depiction of this concept. Note the corresponding dots on the 2D image that are transformed to a position on the roadway.

Several things about the scene represented in the video must be either known or estimated, in order for the transformation to occur. For instance, the geometry of the scene must be known and recorded in a 3D computer environment. Also, some assumptions or determinations must be made about the object being tracked. Specifically, the height off the ground is needed. The reason for this, is that the ray fired from the camera is a straight line headed to the computer environment's background geometry, which is typically a roadway or walkway or ground of some sort. The object being tracked is rarely at ground level, but rather several feet above it. In order to place the object in

3D space correctly, the point along the line will need to match the height off the ground of the actual object being recorded. Figure 5 demonstrates this concept. In this figure, a ray is traced from the camera to the ground, and the height of a tail lamp (the object being tracked in this demonstration) is shown in contact with this line, therefore determining where along the ray trace line the point being transformed into the 3D world should be located. Knowing, or estimating the height of the headlamp, for these purposes, would be needed, otherwise the point when transformed to the 3D world would end up on the ground.

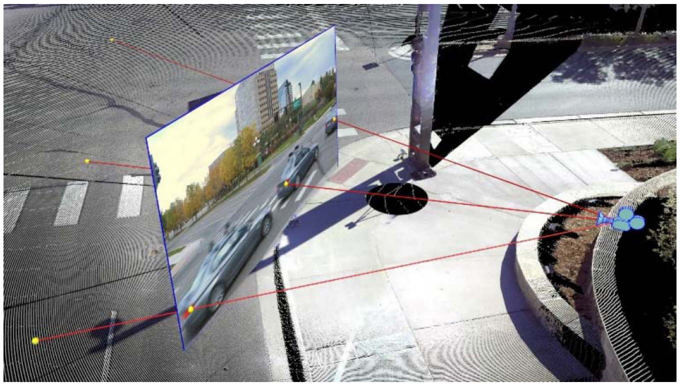

Figure 4. Concept of 2D to 3D transformation

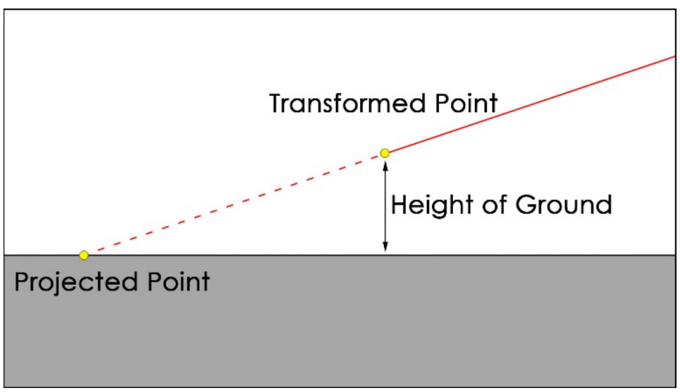

Figure 5. Concept of determining where, along the ray trace line, a point will be located in 3D space

Testing Scenarios

In order to demonstrate this process, and evaluate how accurately the process tracks movement of an object in video, three different testing scenarios were performed. The testing scenarios have different modes of movement, different speeds, and different movement patterns so that the tracking process can be evaluated for a variety of objects being tracked and a variety of path and speeds. Table 1 lists the scenarios that were videotaped and the Resulting data collected through this process.

To evaluate the accuracy at which the 2D transformation process tracks speed and position, the results of the process were compared to a RaceLogic VBOX Data Acquisition Unit that was also tracking the position of the vehicles used in each of the scenarios.

Table 1. Test scenarios and objects to be tracked

Testing Scenario	Processed Results
1-Baby Stroller	Baby Stroller Speed
2-Bicycle Going Straight	Bicycle Path and Speed
3-Bicycle Turning	Bicycle Path and Speed
4-Car Constant Speed	Car Path and Speed
5-Car Starting From Stop	Car Path and Speed
6-Car Turning	Car Path and Speed
7-Pedestrian Walking	Pedestrian Speed

To simplify the camera matching process, and reduce the number of geometry scenes that needed to be created, a single site was utilized for all six of the testing scenarios. Figure 6 is an aerial image that shows the testing intersection, and the location of the camera, denoted in an orange circle, used to record video. Figure 7 shows the same aerial with the path of travel for each of the scenarios denoted. The pedestrian path is in white, the bicycle path is in orange, and the passenger car path is in red. In addition to the mode of travel and the speed, the paths of travel vary in their horizontal and vertical movement as observed in the video, whereby some scenarios have travel paths that go from right to left, some from left to right, and some from top to bottom. This variety is to provide a full range of scenario conditions to evaluate.

Figure 6. Aerial of intersection with camera locations denoted

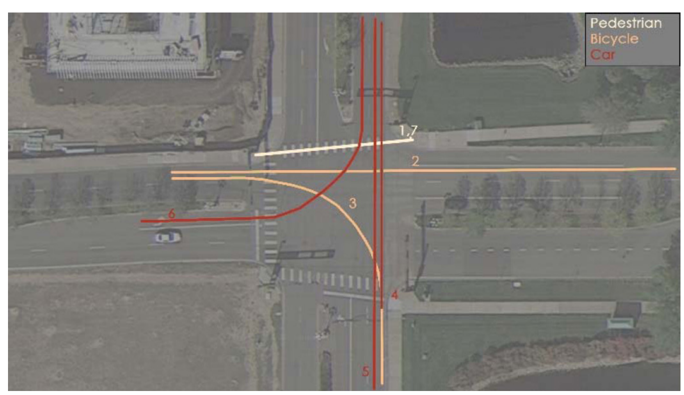

Figure 7. Same aerial with travel paths and scenarios

Procedure

Describe the steps of the procedure, listing them:

1. Collection of geometry of the scene
2. Collection of video footage
3. Collecting VBOX data for comparison
4. Camera Matching Photogrammetry
5. Auto tracking of pixels
6. Transformation of 2D points to 3D environment
7. Adjusting the position along the ray trace
8. Comparison to VBOX tracking

1. Collection of Geometry of the Scene

The area depicted in the image in Figure 6 was digitally mapped using a Sokkia Total station and a Faro Focus 3D Laser scanner so that objects such as the roadway, traffic lights, signs and other objects that would help result in a successful camera match could be recorded. Figure 8 is image of the scan data that resulted from the Faro scan of the scene, and Figure 9 is the scan and survey data processed into surface geometry to be used in camera matching and 3D coordinate transformation.

Figure 8. Results of the scan of the scene

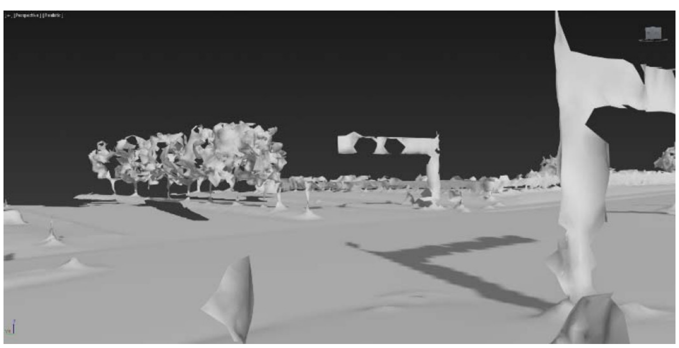

Figure 9. Processed scan data into surface geometry for camera matching and 3D transformation

2. Collection of Video Footage

A total of six scenarios were performed using three different modes of movement. The first run was the slowest, and included a pedestrian walking a baby stroller. The stroller was used in conjunction with the VBOX to obtain a smooth signal at a walking pace. The bicycle represented a faster mode of travel, and two paths of travel were used in this scenario. In one, the cyclist went straight across the intersection, and in the other the cyclist made a turn through the intersection. A passenger car made up the remaining runs, and included three speed changes driving straight through the intersection, and one path of travel that was a turn through the intersection. Figure 10 shows three video frames from each of the six scenarios tested.

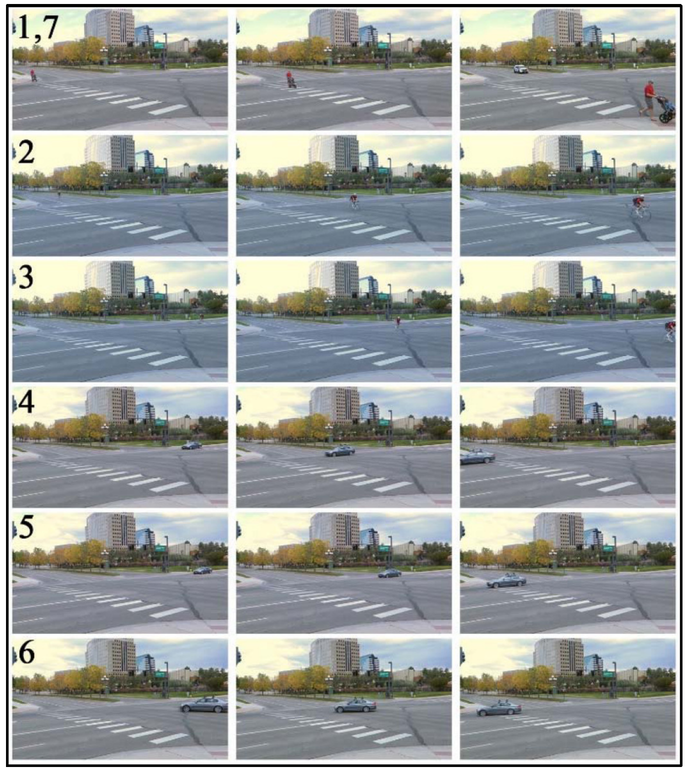

Figure 10. Still frames from video collected for each scenario

3. Collection of VBOX Data for Comparison

Velocity data was collected for each scenario using a Racelogic VBOX VB20SL3 data logger. This data logger measures speed and position through the use of a global positioning system (GPS). The data logger recorded data at 20Hz, and received a GPS signal through a single antenna. The VBOX calculates velocity with an accuracy of 0.1Km/h and resolution of 0.01Km/h. The VBOX calculates velocity from the recorded positions and the VBOX software automatically converts this data to miles per hour for final analysis. The VBOX data was filtered using a five point moving average. This removed the recorded noise at low speeds. The filtering was unnecessary for the tests with the car, but it was used for consistency. Figure 11 shows the mounting of the VBOX unit in a stroller, on the bike and in the car respectively. The Video and VBOX data were linked together by use of a high intensity LED that was mechanically connected to the start button on the VBOX. When the start button for the VBOX was released the LED would turn off at that same moment, thus being a visible point in the video when the run had started in the VBOX.

Figure 11. Photos of VBOX unit mounted in the test scenarios

4. Camera Matching Photogrammetry

The step of Camera Matching Photogrammetry determines the position of the camera with in the 3D environment. The camera's location relative to the stationery background objects in the scene, is determined through this process and Figure 12 and Figure 13 show the results of the camera matching process.

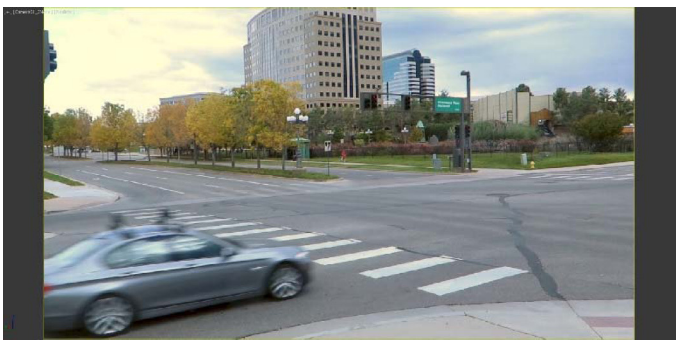

Figure 12. Image and view of the actual camera that was used in the camera matching process.

Figure 13. Camera Matched Camera viewing the computer scene geometry from the same location as actual camera

5. Auto Tracking of Pixels

Each of the video files was imported into the PFTrack[tm] and Adobe After Effects video editing and tracking programs. As part of the tracking process, the video sequence is displayed as a background, and a pixel is selected for tracking. The program allows for the tracking process to analyze three parameters, and these parameters can be selected for best results. Each parameters is one of three deformation properties including skew, scale, and rotate. Scale allows for changes in the size of the pattern, rotate allows for rotation of the pattern and skew allows for deformation of the pattern consistent with changes in perspective. When enabling all three parameters, the auto tracking has the best opportunity to continue tracking the pixel as it changes size and shape throughout the video frames. When the Auto tacking is completed, the results can be visually verified against the actual video Figure 14 shows a still frame of the video capturing the scenario with the bicycle run. A path of points trailing the bicycle denotes the tracking process.

Figure 14. Pixel designated for Auto track

For each scenario, a specific object on each mode of movement was tracked. Table 2 lists the specific pixel object that was tracked in the video, along with the height off the ground that is estimated or determined for that object. If an estimate is required for the height of the object being tracked, getting the estimate as close as possible yields the best results, since estimating a height higher or lower than the object actually is off the ground, will result in a varying positions on the ground. How much the estimate is off, and the effect this would have on the final results depends on several factors including the height of the camera above the object being tracked. This is because a triangle is formed between the camera position, the object being tracked and the resulting position on the ground (see figure 5). In general, estimates that are a few inches off did not have a significant effect on the final results. As an example, in our analysis, changing the height of the estimated positions by a 6 inches resulted in a difference in speed of up to 13 percent. Since the camera is higher than the tracking point making the tracking point higher moves the points closer to the camera. Closer to camera makes the whole path smaller so speed decreases. Moving the point down would have the opposite affect and the speed would increase. The further the point is away from the camera the more it will be affected by changes in height as well. Appendix A has been included to show the matrix of the coordinates that resulted from the tracking process for the bicyclist's helmet.

Table 2. Scenarios and objects to be tracked

Testing Scenario	Tracked Object	Height
1-Baby Stroller	Baby Stroller Seat	26"
2-Bicycle Going Straight	Bicycle Helmet	64"
3-Bicycle Turning	Bicycle Helmet	64"
4-Car Constant Speed	Head Light	30"
5-Car Starting From Stop	Head Light	30"
6-Car Turning	Tail Light	34"
7-Pedestrian Walking	Torso	38"

6. Transformation of 2D Points to 3D Environment

Using the pixel coordinates determined through the tracking process, and in conjunction with the location, vertical and horizontal orientation of the camera relative to the background, and its field of view, ray traces were projected through the coordinates to create points on the ground for each tracked position. This geometrical relationship of the pixel location in the video relative to the corresponding point on the ground is represented in the following:

$$TM = \begin{matrix} [Xx, Yx, Zx, Px] \\ [Xy, Yy, Zy, Py] \\ [Xz, Yz, Zz, Pz] \\ [0\ ,0\ \ ,0\ \ ,1\ ] \end{matrix}$$

$$X = Px - \frac{W}{2}$$

$$Y = Py - \frac{H}{2}$$

$$Z = \frac{-W * FL}{9}$$

$$Pg = [X, Y, Z, 1] * TM$$

(eq. 01)

Where W is the width of the image, H is the height of the image, Px / Py are the 2D coordinates of the object being tracked, FL is the focal length of the camera and TM is the 4x4 transform matrix of the 3D camera. It is comprised of 4 components, 3 vectors representing the X, Y and Z axis of the camera and a 4^{th} component for the position of the camera. These are denoted as X, Y, Z and P in the matrix above. Pg is multiplied by TM yielding the transformed 3D position of the tracked pixel in the computer environment a ray is generated at the origin of the 3D camera with a direction pointing from the camera origin through the solved location of the tracked pixel. That ray is traced through the scene until it intersects with the geometry of the ground resulting in a 3D point at that location.

7. Adjusting the Position Along the Ray Trace

Since the ray trace produces a point on the ground, this point must be adjusted to properly reflect were along the line the actual object being tracked would be located. In the case of the bicycle, the height of the rider's head of the ground was measured at 5.3' feet. Using the following equation, the actual transformed position of the tracked pixel was adjusted along the line and properly located in the 3D environment.

$$P = V \cdot \left(\frac{H}{V \cdot N}\right) + \mathrm{Pg}$$

(eq. 02)

Where Pg is the ground point, V is the normalized vector from Pg to the camera, N is the normalized surface normal off the ground at Pg and H is the height of the object off the ground.

8. Comparison to VBOX Tacking

Since the pixel coordinates are transformed to a 3D environment, a matrix can be created for each position at each frame, and the velocity and acceleration of the object in 3D space then plotted. Figure 15 is a graph of the velocity of the car as it makes a turn through the intersection. Velocity is represented in the Y axis in miles per hour, and the X axis represents time in seconds. In this figure, the tracking from the 2D transformation process is overlaid on the VBOX data. Since the VBOX recorded more movement of the car than is represented in the video frames, the start and end of the 2D tracked velocities are shorter than the VBOX. The 2D tracked velocity closely matches the VBOX velocity. As shown in this figure the speeds calculated have at the highest, a difference of about 0.8 mph.

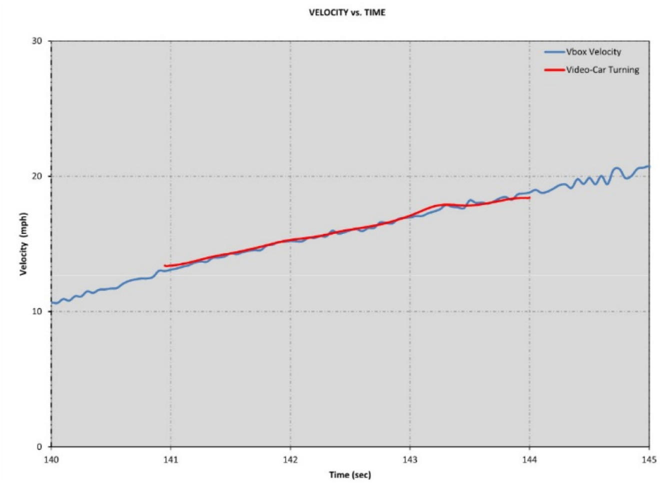

Figure 15. Graph of velocity from the tracking of #6 passenger car turning

The velocities for each of the 2D tracked runs were compared to their respective VBOX recordings. Figures 16, 17, 18, 19, 20, 21 show comparisons of the other 5 scenarios. In Figure 16, one particular section shows misalignment between the tracked velocity and the VBOX data. This is discussed further in the results and summary sections, but worth pointing out as an anomaly. In the video, a bump can be seen occurring at this point in time for the back end of the baby stroller. This bump was not recorded in the VBOX, but manifested as an increase in velocity for the 2D tracked pixel. Since the anomaly is visible in the video, this short section can be ignored by visually analyzing the video and comparing what is observed relative to the output of velocities in the graphs. This area is circled in orange.

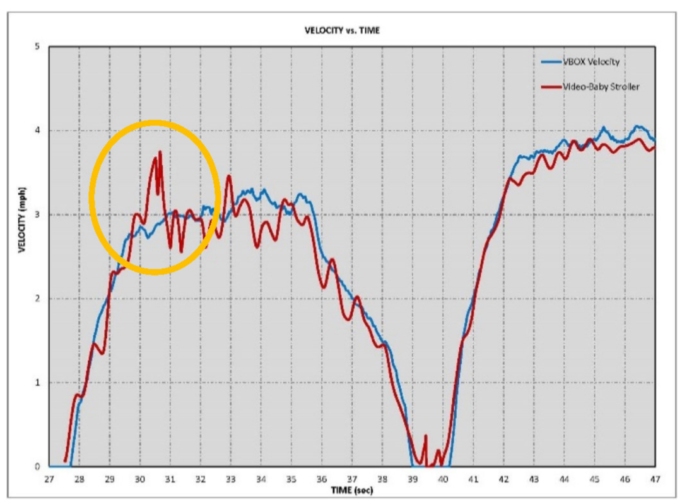

Figure 16. Graph of velocity from #1-baby stroller

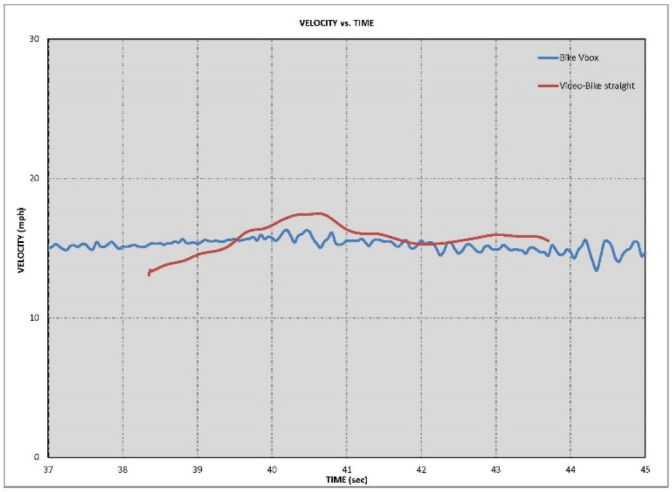

Figure 17. Graph of velocity from #2-bicycle straight

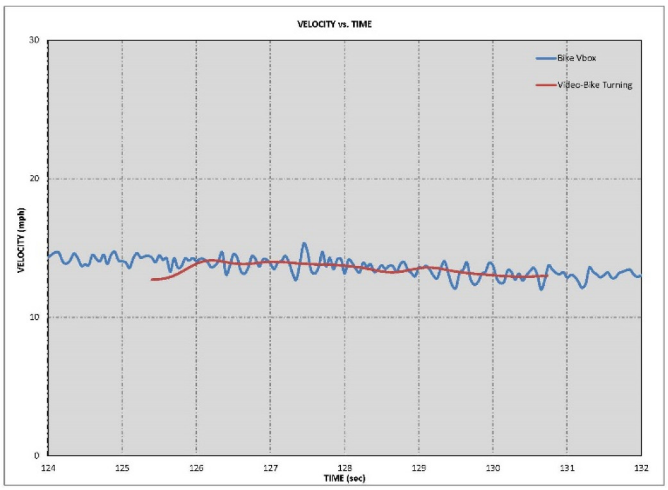

Figure 18. Graph of velocity from #3-bicycle turning

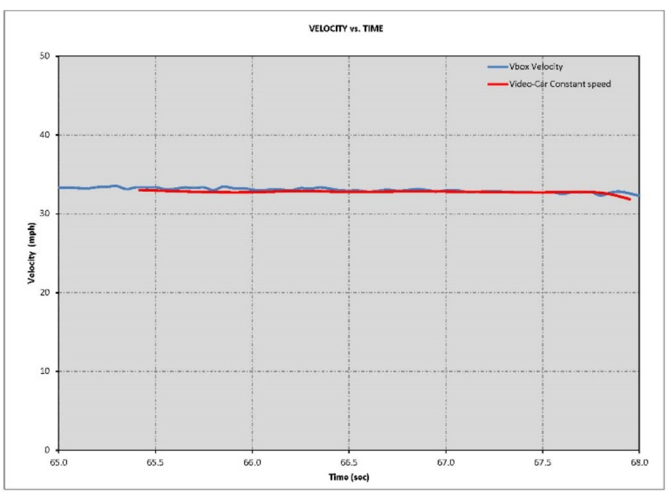

Figure 19. Graph of velocity from #4-car constant speed

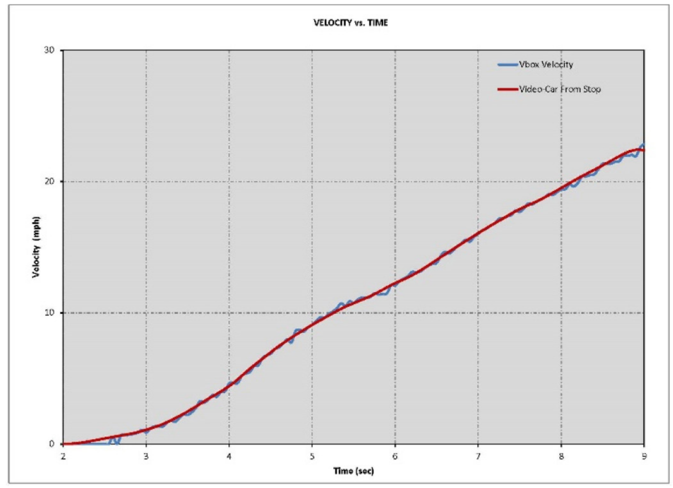

Figure 20. Graph of velocity from #5-car starting from a stop

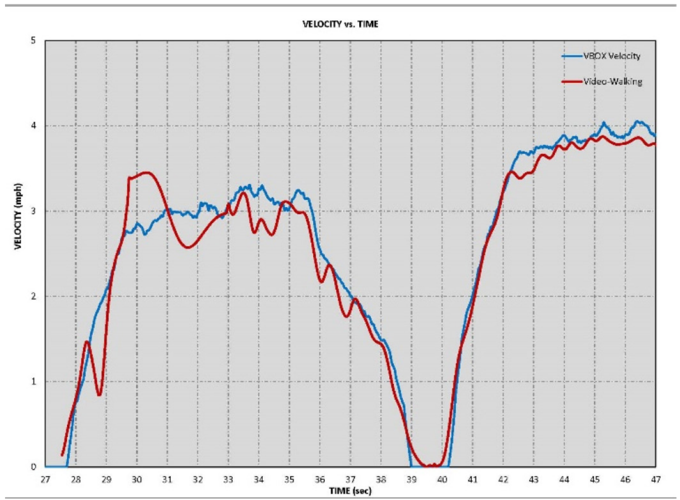

Figure 21. Graph of velocity from #7-pedestrian walking

Results

The speeds of walking, biking, and driving from both the VBOX and the video were compared directly to one another. This was done by outputting the numerical values of the speeds for each scenario and then calculating the acceleration between every two adjacent data points. If this acceleration was larger than one G (32.2 ft/sec^2) the data was excluded. The one G limit was chosen because accelerations larger than one G for the given scenarios are highly unlikely. The sample rate of the Video data was 60Hz and the VBOX was 20Hz, this allowed for a direct comparison of every third sample of the Video Data. This method developed speeds with close representation to the VBOX recorded speed. Table 3 shows the calculated error range for each scenario at any given speed.

Table 3. Error in speed

Testing Scenario	Error in Speed (mph)	Percent Difference
1- Baby Stroller	+0.45, -0.56	17%
2-Bicycle Going Straight	+2.03, -1.88	16%
3-Bicycle Turning	+0.27, -1.61	11%
4-Car Constant Speed	+0.16, -0.75	2%
5-Car Starting From Stop	+0.35, -0.48	2%
6-Car Turning	+0.36, -0.61	3%
7-Pedestrian Walking	+0.72, -0.47	26%

Summary

While the results of the process described in this paper aligned well with the VBOX data, a visual analysis of the video in relation to the data should also be undertaken, since some anomalies observed in the tracking process can easily be explained when watching the video. Large changes in velocity over short times caused by bumps in the surface of the walking/biking/driving path can, through common sense, be found to be unreasonable for use in calculating overall speeds and should be excluded. These bumps are not reflected in the GPS data because of the small changes in the vertical direction over a short time. Making these exclusions reduces the possible difference in speeds from a possible 50% (in the pedestrian tests) to the reported values in Table 3. These values reflect the greatest difference in speed compared to the VBOX and are examining steady state motion of the object being tracked.

Aside from these results, there were some issues related to performing this process. Because the 2D transformation component of this process requires their be an angle between the camera, object being tracked and the ground behind the object, this process is best suited to cameras that are elevated, such as surveillance cameras or in dash cameras on taller vehicles. If for instance, the object being tracked is the same height off the ground as the camera, since there is no ground upon which to trace a ray from the camera, there could be no solution for determining the pixels location. A stationery camera is certainly the easiest condition for tracking objects in video, though a moving camera, such as mounted on a vehicle, or a rotating surveillance camera, could still work in this process assuming that the cameras position and orientation are properly camera matched for each position that the camera changes. This is, again, because video is a series of single frames, and for each frame that is camera matched the position of the target can then be tracked as described in this paper. For accident reconstruction purposes, there are errors present in digital video such as lens distortion, and potential errors from these sources have been discussed and quantified in other publications [9], though accounting for these potential errors is important to ensure the most accurate results.

Another issue that arose, and was represented in slight acceleration and deceleration shifts as seen in Figures 16, occurred when the stroller wheels hit a bump in the road. In this event the 2D tracked pixel would appear to move rapidly up and down for a short period of time (about 1 second). When transformed to the 3D scene, this bump would translate in a lateral position on the road, that would increase and decrease speed. For this reason, it is important to visually review the video when applying the tracking process. If, when the data is output from the track, a sudden, and unexpected acceleration or deceleration is observed, the video should also be analyzed. Looking closely at the frames, it can be determined if this shift is explained by an artifact such as a bump in the road, rather than an actual acceleration or deceleration in real life. If it is an artifact of a bump, this particular section of the data could be modified to better transition between the other sections of the data where there is higher confidence in the velocity that resulted from the tracking.

The same process discussed in this paper would be valid for any instance of digital video, provided an analysis of the frame rate and playback rate of the digital video was considered, and other potential distortion or artifacts that might be inherit in the camera system are also analyzed [9].

Because the tracking of the pixel relies on the ability of the program to distinguish the selected pixel from other pixels, the contrast between the pixel of interest and the surrounding pixels must be maintained. If the contrast of the pixel being tracked is not distinguishable from other pixels, there would be gaps in the tracking. These gaps could be accounted for by assuming a constant change between tracked areas in the absence of other information, but the length of the gap would have an increasing effect on the ramifications of such an assumption.

The tracking process focuses on recording the position of only one pixel. For situations where the speed and position is required of an object in the video that is not rigid, multiple pixels would likely need to be tracked. For instance, in the movement of a person in video, where arms swing, and legs move, individual parts could be tracked to obtain the results needed. Likewise, if the operator of a vehicle moves independent of the vehicle itself, care needs to be taken in which pixel is being tracked to ensure the speed and position is being reported for the correct object of interest.

References

1. Fenton, S., Neale, W., Rose, N., and Hughes, C., "Determining Crash Data Using Camera Matching Photogrammetric Technique," SAE Technical Paper 2001-01-3313, 2001, doi:10.4271/2001-01-3313.
2. Coleman, C., Tandy, D., Colborn, J., and Ault, N., "Applying Camera Matching Methods to Laser Scanned Three Dimensional Scene Data with Comparisons to Other Methods," SAE Technical Paper 2015-01-1416, 2015, doi:10.4271/2015-01-1416.
3. Cliff, W., Maclnnis, D., and Switzer, D., "An Evaluation of Rectified Bitmap 2D Photogrammetry with PC-Rect," SAE Technical Paper 970952, 1997, doi:10.4271/970952.
4. Woolley, R., White, K., Asay, A., and Bready, J., "Determination of Vehicle Crush from Two Photographs and the Use of 3D Displacement Vectors in Accident Reconstruction," SAE Technical Paper 910118, 1991, doi:10.4271/910118.
5. Neale, W., Fenton, S., McFadden, S., and Rose, N., "A Video Tracking Photogrammetry Technique to Survey Roadways for Accident Reconstruction," SAE Technical Paper 2004-01-1221, 2004, doi:10.4271/2004-01-1221.

6. Neale, W., Marr, J., and Hessel, D., "Video Projection Mapping Photogrammetry through Video Tracking," SAE Technical Paper 2013-01-0788, 2013, doi:10.4271/2013-01-0788.
7. Rose, N., Neale, W., Fenton, S., Hessel, D. et al., "A Method to Quantify Vehicle Dynamics and Deformation for Vehicle Rollover Tests Using Camera-Matching Video Analysis," *SAE Int. J. Passeng. Cars - Mech. Syst.* 1(1):301-317, 2009, doi:10.4271/2008-01-0350.
8. PFtrack, After Effects, NukeX, Shake, 3D Equilizer, SynthEyes, Fusion
9. Neale, W., Hessel, D., and Terpstra, T., "Photogrammetric Measurement Error Associated with Lens Distortion," SAE Technical Paper 2011-01-0286, 2011, doi:10.4271/2011-01-0286.

Contact Information

William Neale, M. Arch.
Kineticorp, LLC
(303) 733-1888
wneale@kineticorp.com
www.kineticorp.com

APPENDIX

Appendix A

Frame	X	Y	Simularity
9642	69.03745	596.3848	0.799661
9643	69.0334	596.3788	0.78863
9644	69.57579	596.1879	0.804223
9645	69.591	596.1787	0.795219
9646	69.60156	596.1749	0.790786
9647	70.50862	596.0931	0.803905
9648	70.55214	596.079	0.801717
9649	71.51148	595.9424	0.836485
9650	71.51984	595.9376	0.824058
9651	72.45194	595.8503	0.85427
9652	72.55598	595.8215	0.855522
9653	72.6396	595.783	0.85064
9654	72.65584	595.7782	0.846297
9655	73.67096	595.79	0.846039
9656	73.88258	595.7886	0.847457
9657	74.62474	595.8124	0.82368
9658	75.32336	595.9237	0.796106
9659	75.31803	595.9254	0.787634
9660	75.21478	595.9445	0.768699
9661	75.63773	595.978	0.759958
9662	76.00369	596.0106	0.765294
9663	75.98963	596.009	0.732153
9664	76.31901	596.0463	0.740036
9665	76.76836	596.0151	0.75113
9666	76.74161	596.0132	0.726198
9667	77.17963	595.9819	0.753896
9668	77.15454	595.9784	0.743911
9669	77.37414	595.9273	0.763303
9670	77.34479	595.9236	0.742777
9671	77.88226	595.8875	0.755281
9672	77.84726	595.8796	0.747203
9673	78.79502	595.8716	0.782263
9674	78.77586	595.8625	0.771324
9675	79.58405	595.8007	0.798168
9676	79.58787	595.791	0.792548
9677	79.58907	595.782	0.77367
9678	80.37914	595.6573	0.792025
9679	80.39269	595.6523	0.802319
9680	80.94624	595.5068	0.813491
9681	81.72846	595.3468	0.819032
9682	81.78017	595.321	0.822387
9683	82.92036	595.0994	0.823705
9684	83.17682	594.9805	0.809056
9685	83.23291	594.9513	0.812499
9686	84.22996	594.7225	0.816939
9687	84.33127	594.6477	0.834971
9688	85.33472	594.6256	0.849006
9689	85.43131	594.5587	0.867656
9690	86.42042	594.5421	0.87027
9691	86.63366	594.5175	0.870833
9692	86.77342	594.4439	0.864137
9693	87.00187	594.3857	0.869877
9694	87.00941	594.3849	0.868348
9695	87.89289	594.3623	0.866943
9696	88.28667	594.3524	0.870553
9697	88.3056	594.3492	0.872355
9698	89.09896	594.2792	0.873399
9699	89.10072	594.2801	0.86666
9700	89.66055	594.3148	0.854004
9701	89.65758	594.3168	0.852669
9702	90.1133	594.3459	0.832296
9703	90.45786	594.3923	0.807317
9704	91.42955	594.3959	0.799637
9705	91.43346	594.3784	0.809224
9706	92.25996	594.3431	0.805173
9707	92.30881	594.3267	0.80964
9708	92.29732	594.3212	0.814319
9709	92.42517	594.1619	0.819578
9710	92.4017	594.142	0.807226
9711	93.14615	594.1071	0.823793
9712	93.14285	594.0954	0.825253
9713	93.87427	594.0361	0.843958
9714	93.88107	594.03	0.834475
9715	94.4702	593.8154	0.856358
9716	94.52185	593.7168	0.853355
9717	95.53432	593.6784	0.889207
9718	95.56345	593.6696	0.895949
9719	96.55448	593.6362	0.940186
9720	96.81307	593.5739	0.945873
9721	97.70565	593.5719	0.956327
9722	97.74867	593.5696	0.953926
9723	98.43648	593.5844	0.976954
9724	98.60376	593.6158	0.970153

9725	98.81413	593.5992	0.758021
9726	98.80971	593.5947	0.766787
9727	99.73064	593.5754	0.755087
9728	100.726	593.5737	0.742072
9729	100.7253	593.5704	0.771228
9730	101.717	593.5663	0.736781
9731	101.7349	593.5704	0.755875
9732	101.7097	593.521	0.784764
9733	101.6292	593.4317	0.824322
9734	101.619	593.4294	0.847225
9735	102.6041	593.4271	0.854405
9736	102.6082	593.4303	0.861904
9737	103.4644	593.4365	0.887636
9738	103.7237	593.4266	0.906485
9739	103.8691	593.3459	0.92894
9740	104.0476	593.3172	0.931126
9741	104.0998	593.3062	0.933673
9742	104.8918	593.2524	0.919709
9743	105.1521	593.2853	0.954066
9744	105.7857	593.247	0.716233
9745	106.7611	593.2465	0.724552
9746	106.6929	593.1925	0.7319
9747	107.6428	593.1857	0.726064
9748	107.6727	593.1366	0.732939
9749	107.6681	593.1033	0.748249
9750	108.2958	593.0649	0.768148
9751	108.37	593.0538	0.798575
9752	109.2098	593.0919	0.848548
9753	109.5613	593.035	0.87837
9754	109.9109	592.9207	0.935556
9755	110.0483	592.8967	1
9756	110.571	592.8702	-1
9757	111.4927	592.8202	-1
9758	112.2929	592.7205	-1
9759	113.1313	592.6456	-1
9760	114.4733	592.5758	-1
9761	115.1945	592.5237	0.82824
9762	115.2369	592.4702	0.834566
9763	116.1108	592.4406	0.838811
9764	116.1659	592.4114	0.858939
9765	116.9442	592.3882	0.854742
9766	116.9858	592.3914	0.862613
9767	117.7036	592.3495	0.850815

9768	118.0161	592.3018	0.835648
9769	118.8418	592.2194	0.833678
9770	119.2668	592.2096	0.81955
9771	119.438	592.1989	0.80078
9772	119.4305	592.0851	0.77727
9773	120.4016	592.0526	0.766941
9774	120.5243	592.0084	0.752729
9775	121.5088	591.967	0.747993
9776	121.5245	591.9357	0.731074
9777	122.5137	591.9272	0.742101
9778	123.5024	591.9209	0.726819
9779	123.4955	591.9138	0.723448
9780	124.4809	591.9059	0.733585
9781	124.4673	591.8477	0.735888
9782	125.4076	591.8164	0.751917
9783	125.5915	591.6918	0.787913
9784	126.532	591.6838	0.795991
9785	126.6248	591.6622	0.788702
9786	127.5162	591.4727	0.801913
9787	128.532	591.4569	0.805191
9788	128.5553	591.4501	0.814217
9789	129.5555	591.4512	0.833052
9790	129.6009	591.4484	0.849414
9791	130.6038	591.4477	0.840776
9792	130.7424	591.3919	0.860478
9793	131.7305	591.3896	0.877461
9794	131.8593	591.3583	0.893404
9795	132.7488	591.3387	0.914622
9796	132.8095	591.3527	0.942259
9797	133.4842	591.3471	0.947628
9798	133.7635	591.3164	0.969324
9799	134.0855	591.2768	0.71447
9800	135.068	591.2448	0.71666
9801	135.2922	591.1011	0.729774
9802	136.2426	591.0654	0.715135
9803	136.2697	591.0463	0.732938
9804	137.2132	591.0128	0.739649
9805	137.2714	590.9808	0.760789
9806	138.2285	590.9476	0.716657
9807	138.3275	590.9332	0.734239
9808	139.2732	590.9	0.759538
9809	140.263	590.8868	0.739
9810	140.4068	590.8355	0.744912

9811	141.4017	590.8355	0.747194
9812	141.5623	590.7751	0.780414
9813	142.5582	590.775	0.779501
9814	142.7133	590.7437	0.774718
9815	143.6446	590.7653	0.778498
9816	144.6737	590.7626	0.783078
9817	144.8996	590.7052	0.791593
9818	145.6681	590.5997	0.79466
9819	146.6613	590.5947	0.783673
9820	146.7608	590.5503	0.817412
9821	147.7497	590.5418	0.819546
9822	147.8625	590.5117	0.821964
9823	148.7736	590.496	0.834162
9824	149.7478	590.4765	0.835925
9825	149.9525	590.3833	0.814557
9826	150.7611	590.3839	0.805673
9827	151.7222	590.3663	0.828588
9828	151.797	590.3685	0.850275
9829	152.4649	590.3419	0.852348
9830	153.3444	590.3193	0.845567
9831	153.6313	590.316	0.850691
9832	154.5909	590.3361	0.869185
9833	154.8469	590.2849	0.85834
9834	155.5147	590.2634	0.851062
9835	156.3746	590.2628	0.872105
9836	156.5724	590.2549	0.892215
9837	157.2701	590.1891	0.879431
9838	157.4975	590.1919	0.869297
9839	158.2399	590.1755	0.870045
9840	159.1001	590.1452	0.863238
9841	159.7757	589.9991	0.844712
9842	160.5063	589.928	0.829464
9843	161.4083	589.8723	0.844132
9844	161.5735	589.8225	0.863943
9845	162.51	589.7005	0.843739
9846	162.7465	589.637	0.830271
9847	163.4976	589.605	0.847303
9848	164.2166	589.4366	0.830548
9849	164.9049	589.2559	0.785609
9850	165.7101	589.1962	0.805311
9851	166.4997	589.1073	0.807531
9852	167.4415	589.0379	0.785665
9853	167.5522	588.984	0.791403

9854	168.3051	588.9345	0.80637
9855	169.2879	588.9163	0.799879
9856	170.3214	588.9091	0.7856
9857	170.4796	588.8563	0.795651
9858	171.3685	588.766	0.801174
9859	172.3671	588.7515	0.801117
9860	172.4407	588.6814	0.820133
9861	173.42	588.6647	0.822978
9862	173.6369	588.6501	0.834622
9863	174.4316	588.5956	0.836357
9864	175.2317	588.4822	0.835654
9865	176.0727	588.4138	0.851242
9866	177.0465	588.3943	0.848638
9867	178.0114	588.364	0.868374
9868	178.1832	588.3287	0.895162
9869	178.9044	588.2893	0.898491
9870	179.7903	588.1862	0.91833
9871	180.041	588.1782	0.91148
9872	180.7075	588.0905	0.953848
9873	181.4148	588.0636	0.727051
9874	182.1307	587.9918	0.739404
9875	182.6254	587.8524	0.7119
9876	183.4929	587.7974	0.71476
9877	183.4865	587.7855	0.732284
9878	184.2839	587.7672	0.738304
9879	185.0284	587.7625	0.744292
9880	185.9199	587.7516	0.777274
9881	186.7556	587.7447	0.778602
9882	187.749	587.7444	0.777043
9883	187.7583	587.7451	0.772933
9884	188.5226	587.6987	0.783931
9885	189.4738	587.6865	0.781281
9886	189.4738	587.6833	0.777277
9887	190.2135	587.6342	0.786419
9888	191.1359	587.6261	0.809525
9889	191.7888	587.5452	0.815414
9890	192.5008	587.4952	0.815217
9891	193.4902	587.4954	0.839768
9892	194.2793	587.5379	0.851822
9893	194.5607	587.4749	0.827861
9894	195.4489	587.5113	0.816877
9895	195.6076	587.4953	0.758696
9896	197.0608	587.5766	0.713315

9897	197.8329	587.4706	0.703756
9898	198.7556	587.4324	0.704896
9899	199.7417	587.4134	0.727859
9900	199.7437	587.4095	0.766356
9901	200.4871	587.4114	0.773415
9902	201.3993	587.4177	0.777164
9903	202.0865	587.3724	0.783665
9904	203.0013	587.3698	0.777717
9905	203.9368	587.3631	0.807502
9906	204.6901	587.3383	0.81185
9907	205.4324	587.3389	0.81496
9908	206.4102	587.3344	0.801948
9909	206.4907	587.3167	0.827769
9910	207.0809	587.2406	0.821127
9911	207.6303	587.1268	0.801095
9912	208.6156	587.1213	0.836008
9913	209.5614	587.0942	0.857475
9914	209.591	587.1109	0.847661
9915	210.3798	587.1349	0.870769
9916	210.9761	587.13	0.87996
9917	211.5323	587.0767	0.870727
9918	212.2268	587.0604	0.883517
9919	212.9673	587.0703	0.894967
9920	213.7054	587.0795	0.883902
9921	214.3472	586.9966	0.900703
9922	214.986	586.984	0.89408
9923	215.6916	586.9784	0.894825
9924	216.3361	586.9617	0.901931
9925	216.7685	586.9317	0.897363
9926	217.4593	586.8556	0.921749
9927	218.4117	586.8478	0.942512
9928	219.2827	586.8408	0.71143
9929	220.1037	586.8351	0.739393
9930	220.9974	586.8324	0.77346
9931	221.7592	586.7621	0.777449
9932	221.7361	586.705	0.816646
9933	222.4637	586.6072	0.821753
9934	223.4341	586.5668	0.816272
9935	223.5345	586.5458	0.871107
9936	224.5249	586.5444	0.883714
9937	225.5023	586.5266	0.953511
9938	225.9153	586.429	0.701186
9939	226.8378	586.4143	0.75709

9940	226.9291	586.332	0.826039
9941	227.6169	586.2875	0.871093
9942	227.8313	586.2399	0.922551
9943	228.5863	586.2005	0.707742
9944	229.6428	586.1927	0.720308
9945	229.7948	586.1281	0.77773
9946	230.6561	586.063	0.819347
9947	231.6456	586.0498	0.885074
9948	231.8933	586.0361	0.948878
9949	232.246	585.9771	1
9950	233.3397	585.9172	-1
9951	234.4125	585.889	-1
9952	235.1846	585.8823	-1
9953	236.2637	585.7636	-1
9954	237.3427	585.7369	-1
9955	237.9304	585.6966	0.77085
9956	238.888	585.6269	0.790411
9957	239.1683	585.6	0.806361
9958	239.91	585.5336	0.799251
9959	240.7613	585.5331	0.802362
9960	241.6587	585.4988	0.811083
9961	242.5552	585.464	0.81137
9962	243.2969	585.4488	0.812431
9963	244.1268	585.4124	0.817134
9964	244.8583	585.2695	0.817017
9965	245.7408	585.2171	0.81666
9966	246.3848	585.2672	0.81988
9967	247.3054	585.2658	0.829611
9968	248.1544	585.2631	0.820721
9969	248.9874	585.1942	0.826952
9970	249.8165	585.1064	0.821536
9971	250.551	585.0678	0.834144
9972	251.2865	584.9712	0.824283
9973	252.0052	584.8849	0.815892
9974	252.7885	584.7823	0.820203
9975	253.5969	584.6825	0.823973
9976	254.4771	584.6179	0.820978
9977	255.2959	584.5244	0.816702
9978	256.268	584.4979	0.823373
9979	257.2662	584.3546	0.814648
9980	257.4617	584.27	0.807754
9981	258.2958	584.1995	0.815497
9982	258.947	584.0703	0.801253

9983	259.7204	584.0611	0.804916
9984	260.7101	584.0592	0.822512
9985	261.397	583.8791	0.819066
9986	262.3042	583.793	0.816643
9987	263.3019	583.7833	0.825035
9988	263.5864	583.6437	0.816209
9989	264.2777	583.5904	0.827663
9990	265.0039	583.5368	0.820436
9991	265.8215	583.5235	0.80878
9992	266.7088	583.5713	0.793571
9993	267.5876	583.5392	0.772132
9994	268.4616	583.4874	0.750988
9995	269.2353	583.3339	0.740811
9996	270.2156	583.3146	0.720488
9997	270.4139	583.278	0.753049
9998	271.1115	583.1868	0.778259
9999	271.8448	583.1063	0.788371
10000	272.8411	583.1041	0.81164
10001	273.5959	582.9845	0.832196
10002	274.5274	582.9182	0.837437
10003	275.536	582.9003	0.853857
10004	275.8225	582.8614	0.857695
10005	276.5712	582.7627	0.871476
10006	277.3274	582.6855	0.857842
10007	278.2841	582.65	0.873437
10008	279.255	582.618	0.868457
10009	280.2602	582.5909	0.870966
10010	280.5441	582.5194	0.889892
10011	281.4552	582.4314	0.910062
10012	282.4433	582.4084	0.938626
10013	282.7825	582.3396	0.971205
10014	283.5746	582.2191	0.968425
10015	284.5291	582.1617	0.971253
10016	285.3665	582.1931	0.705631
10017	286.2527	582.124	0.71003
10018	286.8372	581.8325	0.703081
10019	287.7992	581.811	0.71364
10020	288.5387	581.6773	0.715316
10021	289.3366	581.5264	0.712538
10022	290.0576	581.3486	0.717413
10023	290.8923	581.2233	0.725011
10024	291.8202	581.1738	0.725728
10025	292.5952	581.0441	0.729825

10026	293.4215	580.9572	0.731974
10027	294.2412	580.9403	0.740983
10028	294.9943	580.8083	0.749316
10029	295.6464	580.6511	0.757524
10030	296.6128	580.627	0.775644
10031	297.4674	580.5508	0.763905
10032	298.3941	580.5174	0.767797
10033	299.2594	580.439	0.760538
10034	300.1526	580.3868	0.757586
10035	300.8014	580.2076	0.766419
10036	301.6944	580.1577	0.773581
10037	302.467	580.0693	0.767948
10038	303.1801	579.9384	0.765176
10039	304.1348	579.8948	0.761445
10040	305.1179	579.8833	0.762627
10041	305.8297	579.7319	0.732485
10042	306.79	579.7231	0.73154
10043	307.7616	579.7226	0.735195
10044	308.7556	579.7238	0.71522
10045	309.7567	579.7373	0.719103
10046	309.825	578.8853	0.742881
10047	310.8003	578.8668	0.743241
10048	311.7356	578.8248	0.745974
10049	312.6849	578.7896	0.745891
10050	313.6211	578.7529	0.755382
10051	314.5346	578.7153	0.759132
10052	315.4781	578.6747	0.758718
10053	316.3852	578.5959	0.762268
10054	317.2498	578.4982	0.757248
10055	318.2395	578.4714	0.750992
10056	319.1827	578.3976	0.759183
10057	319.9579	578.2386	0.763497
10058	320.9137	578.1879	0.766127
10059	321.7964	578.0641	0.767072
10060	322.7251	578.0259	0.765697
10061	323.6448	577.9718	0.76017
10062	324.5327	577.8844	0.754675
10063	325.4651	577.866	0.749543
10064	326.3444	577.8036	0.742559
10065	327.2657	577.7642	0.73284
10066	328.0416	577.6056	0.722322
10067	328.8918	577.5083	0.722797
10068	329.7786	577.4419	0.71977

10069	330.71	577.3976	0.729053
10070	331.5394	577.2803	0.723147
10071	332.5042	577.2334	0.730636
10072	333.4935	577.2075	0.743886
10073	334.2994	577.0486	0.750351
10074	335.186	576.9169	0.756212
10075	336.1628	576.8668	0.748464
10076	336.8716	576.7142	0.757234
10077	337.7602	576.5499	0.762623
10078	338.7303	576.485	0.763952
10079	339.6517	576.4019	0.772245
10080	340.6395	576.386	0.780413
10081	341.587	576.2916	0.792243
10082	342.5457	576.2516	0.799266
10083	343.3854	575.9874	0.794902
10084	344.3888	575.9598	0.827796
10085	345.3881	575.9453	0.825373
10086	345.7101	575.8542	0.849287
10087	346.6937	575.8341	0.870107
10088	347.6411	575.8029	0.877848
10089	348.5544	575.7739	0.905003
10090	349.5123	575.7486	0.918522
10091	350.4829	575.6641	0.930384
10092	351.3974	575.6343	0.93695
10093	352.3327	575.5513	0.959858
10094	353.3276	575.5013	0.974294
10095	354.2981	575.4072	0.976249
10096	355.287	575.3676	0.701525
10097	356.3243	575.3005	0.710847
10098	357.3564	575.1592	0.711428
10099	358.3861	575.0316	0.716252
10100	359.3946	574.9933	0.715664
10101	360.4255	574.795	0.714311
10102	361.4709	574.6647	0.707853
10103	362.5161	574.5739	0.710015
10104	363.5917	574.4071	0.709749
10105	364.7025	574.1388	0.701547
10106	365.7632	573.9617	0.715045
10107	366.8256	573.8212	0.714702
10108	367.8433	573.6937	0.711271
10109	368.8315	573.5929	0.710791
10110	369.7403	573.3253	0.717626
10111	370.7433	573.1	0.715248

10112	371.7261	573.0629	0.724108
10113	373.5967	572.8624	0.745691
10114	374.6801	572.6363	0.751303
10115	375.8263	572.4219	0.759965
10116	376.8696	572.1974	0.75765
10117	377.8415	571.9459	0.746036
10118	378.8372	571.9368	0.728973
10119	380.7005	571.8108	0.738741
10120	381.8237	571.7572	0.738477
10121	383.05	571.5801	0.752104
10122	384.2132	571.403	0.750608
10123	385.1203	571.2235	0.738581
10124	386.9997	571.1699	0.73501
10125	388.1491	570.9178	0.721151
10126	389.2363	570.6581	0.718901
10127	390.2041	570.5276	0.716506
10128	392.1622	570.475	0.733426
10129	393.3476	570.3762	0.741443
10130	394.6741	570.2251	0.75187
10131	395.9088	569.9404	0.753413
10132	396.9132	569.8867	0.743251
10133	398.8276	569.8284	0.738672
10134	400.0005	569.7225	0.735918
10135	401.2671	569.512	0.746342
10136	402.3387	569.4068	0.749238
10137	404.2086	569.2607	0.750519
10138	405.475	569.087	0.766229
10139	406.5974	568.8602	0.758822
10140	408.3532	568.6229	0.750572
10141	409.4972	568.3826	0.746405
10142	410.506	568.2162	0.743053
10143	412.4058	568.1027	0.760496
10144	413.4091	568.0897	0.75625
10145	415.3155	567.9965	0.761674
10146	416.4058	567.894	0.76778
10147	418.2541	567.8127	0.77213
10148	419.4755	567.7667	0.770177
10149	420.4908	567.7218	0.750409
10150	422.3706	567.6475	0.757756
10151	423.4144	567.5977	0.76029
10152	425.3263	567.5859	0.748891
10153	426.4538	567.5113	0.747655
10154	428.3615	567.4685	0.757307

10155	429.6655	567.2471	0.744585
10156	431.6196	567.2213	0.733923
10157	432.8459	567.0377	0.729025
10158	434.7763	566.9721	0.724454
10159	436.0981	566.6403	0.725439
10160	438.0898	566.6158	0.733184
10161	439.2077	566.5166	0.738901
10162	441.1284	566.4314	0.746611
10163	442.1279	566.2891	0.727943
10164	444.0803	566.2716	0.725464
10165	446.0659	566.2637	0.719847
10166	447.3808	566.2327	0.719416
10167	448.6204	565.6806	0.742245
10168	450.4652	565.5293	0.757965
10169	452.4521	565.504	0.761142
10170	453.7012	565.2579	0.760354
10171	455.5547	565.0738	0.772546
10172	457.547	565.0618	0.774435
10173	458.6238	564.8259	0.779742
10174	460.5136	564.6669	0.788268
10175	462.51	564.6604	0.781628
10176	463.8618	564.5541	0.783276
10177	465.7353	564.5054	0.80618
10178	467.5092	564.3997	0.798728
10179	469.2742	564.2817	0.801945
10180	471.0094	564.0623	0.817069
10181	473.0029	564.0565	0.818026
10182	474.4588	563.4359	0.857659
10183	476.2883	563.2198	0.880795
10184	478.1284	562.9576	0.889304
10185	480.0782	562.7783	0.880941
10186	482.0207	562.6351	0.87712
10187	483.8555	562.4253	0.865626
10188	485.7551	562.4357	0.850078
10189	487.6428	561.7272	0.850274
10190	489.6516	561.6229	0.866969
10191	491.6946	561.4009	0.887527
10192	493.7179	561.2816	0.912969
10193	495.857	561.0676	0.950499
10194	498.0408	560.909	0.701045
10195	500.1584	560.5891	0.715849
10196	502.2199	560.4357	0.722237
10197	504.3576	560.1918	0.727717
10198	506.5078	559.819	0.723905
10199	508.587	559.666	0.745236
10200	510.8834	559.3568	0.766482
10201	513.0041	559.1959	0.802672
10202	515.2651	558.5024	0.820237
10203	517.3897	558.2454	0.839049
10204	519.4509	558.1744	0.85134
10205	521.6039	557.5687	0.839587
10206	523.7601	557.0888	0.828733
10207	525.9932	556.6165	0.836185
10208	528.1474	556.3749	0.831585
10209	530.4604	556.0504	0.812985
10210	532.6382	555.6843	0.807128
10211	534.8527	555.2586	0.784212
10212	536.8771	554.923	0.772805
10213	539.4799	554.5681	0.789532
10214	541.5437	554.4451	0.786365
10215	544.2307	554.2444	0.778729
10216	546.3961	554.0384	0.791733
10217	549.0513	553.8268	0.797983
10218	551.206	553.5605	0.780914
10219	553.9598	553.3176	0.768491
10220	556.1909	552.9766	0.770835
10221	558.916	552.624	0.775769
10222	561.11	552.3716	0.783204
10223	563.9105	552.2107	0.792096
10224	566.7012	551.9408	0.810858
10225	569.0522	551.7471	0.819284
10226	571.6966	551.5987	0.825489
10227	574.2933	551.4109	0.838189
10228	576.8859	551.1865	0.831297
10229	579.7243	551.0112	0.858468
10230	582.1247	550.6968	0.86868
10231	584.8512	550.4601	0.880998
10232	587.6047	550.2275	0.905225
10233	590.3463	549.9482	0.948256
10234	593.1891	549.833	0.720365
10235	595.9581	549.5267	0.735282
10236	598.7761	549.4026	0.746198
10237	601.6568	549.2703	0.753862
10238	604.5327	548.953	0.751356
10239	607.4195	548.7297	0.744912
10240	610.3597	548.6468	0.738105

10241	613.3085	548.6033	0.737796
10242	616.2795	548.5943	0.734102
10243	619.177	548.6705	0.739912
10244	622.0403	548.8102	0.747735
10245	624.9608	548.9066	0.771416
10246	627.861	549.0518	0.776269
10247	630.7445	549.1985	0.787927
10248	633.5742	549.4209	0.784726
10249	636.5241	549.7574	0.768091
10250	639.6176	550.1263	0.737439
10251	642.6663	550.3502	0.739186
10252	645.8049	550.5082	0.756693
10253	648.9572	550.7175	0.765007
10254	652.3627	550.9351	0.775637
10255	655.5639	551.0564	0.788181
10256	658.8655	551.2725	0.811961
10257	661.8946	551.4402	0.820175
10258	665.6434	551.4363	0.82535
10259	668.896	551.4683	0.82693
10260	672.1731	551.425	0.83493
10261	675.3749	551.3849	0.827394
10262	678.7536	551.2136	0.791287
10263	681.8742	551.1526	0.777529
10264	685.1877	550.9778	0.766035
10265	688.41	550.7285	0.758495
10266	691.4358	550.6757	0.776098
10267	695.1056	550.4387	0.770524
10268	698.2344	550.3412	0.794307
10269	701.5562	550.096	0.782701
10270	704.8808	549.8562	0.772166
10271	708.1653	549.606	0.772609
10272	711.4405	549.3427	0.808266
10273	714.7543	549.0505	0.8124
10274	717.8564	548.9803	0.816904
10275	721.6502	548.8793	0.818087
10276	724.7177	548.8435	0.819501
10277	728.5027	548.7607	0.826194
10278	731.8513	548.6625	0.816559
10279	734.8853	548.6241	0.823661
10280	738.7905	548.5829	0.803478
10281	741.8955	548.578	0.801703
10282	745.7074	548.5657	0.809188
10283	748.8464	548.5629	0.79441

10284	752.6884	548.5485	0.791746
10285	755.9885	548.4954	0.79398
10286	759.9755	548.4882	0.772099
10287	763.0278	548.4648	0.736617
10288	766.8754	548.3802	0.735411
10289	770.8771	548.3779	0.759992
10290	774.115	548.288	0.792885
10291	778.0726	548.2563	0.795407
10292	781.9606	548.2626	0.813481
10293	785.897	548.1971	0.786198
10294	789.205	548.0781	0.766265
10295	793.1746	548.0579	0.773726
10296	797.0898	547.9716	0.780701
10297	801.1009	547.9424	0.788342
10298	805.105	547.8809	0.791262
10299	809.0311	547.6656	0.798422
10300	813.0429	547.5513	0.774219
10301	817.1129	547.4266	0.768973
10302	821.2021	547.2344	0.778122
10303	825.2715	547.1147	0.810854
10304	829.4597	546.9619	0.836352
10305	833.6462	546.8565	0.857255
10306	837.6875	546.8066	0.921344
10307	841.7394	546.7842	0.709078
10308	846.2271	546.7562	0.713941
10309	849.9706	546.7378	0.728506
10310	854.2814	546.7368	0.737206
10311	858.8332	546.7366	0.741779
10312	862.5868	546.7223	0.773712
10313	866.9407	546.7022	0.777963
10314	871.2381	546.6974	0.777876
10315	875.6017	546.7047	0.775945
10316	880.0269	546.6938	0.777037
10317	884.4581	546.682	0.779784
10318	888.9223	546.6554	0.786023
10319	893.3555	546.6082	0.785581
10320	897.8934	546.5892	0.794802
10321	902.3925	546.5645	0.797352
10322	906.9564	546.5563	0.758473
10323	911.4316	546.5158	0.766601
10324	915.9666	546.4871	0.785428
10325	920.582	546.4662	0.780926
10326	925.1868	546.4527	0.797431

10327	929.7628	546.4522	0.777074
10328	934.4042	546.468	0.792261
10329	939.0837	546.5098	0.808617
10330	943.8619	546.547	0.818297
10331	948.6348	546.5829	0.810497
10332	953.4128	546.6514	0.805934
10333	958.085	546.6711	0.816703
10334	963.3139	546.7012	0.816164
10335	968.1282	546.6819	0.826664
10336	973.0362	546.6215	0.836573
10337	978.3076	546.5237	0.848673
10338	983.545	546.4166	0.875583
10339	988.7633	546.3521	0.883689
10340	993.7123	546.1857	0.890376
10341	998.9554	546.1096	0.896917
10342	1004.212	545.9711	0.895457
10343	1009.445	545.805	0.895641
10344	1014.784	545.6149	0.867775
10345	1020.041	545.5052	0.868349
10346	1025.515	545.3532	0.852099
10347	1030.819	545.2567	0.851817
10348	1036.581	544.7705	0.863529
10349	1041.859	544.6218	0.881593
10350	1047.639	544.3938	0.923041
10351	1053.34	544.1741	0.949562
10352	1059.181	544.0884	0.959563
10353	1064.897	543.8691	0.704059
10354	1070.801	543.7247	0.71102
10355	1076.799	543.6681	0.710124
10356	1082.812	543.5756	0.720998
10357	1088.836	543.4879	0.727065
10358	1094.909	543.2943	0.730221
10359	1101.042	543.0767	0.739636
10360	1107.157	542.7005	0.732103
10361	1113.312	542.6326	0.740047
10362	1119.599	542.3602	0.753317
10363	1125.904	542.1761	0.751462
10364	1132.286	542.079	0.75217
10365	1138.813	541.8369	0.75664
10366	1145.32	541.5363	0.758756
10367	1152.278	541.3044	0.75452
10368	1159.212	541.0068	0.751186
10369	1165.634	540.7179	0.783493
10370	1172.633	540.6057	0.798736
10371	1180.029	540.4702	0.803955
10372	1186.891	540.3676	0.810315
10373	1193.751	540.2033	0.817247
10374	1201.14	539.8824	0.815003
10375	1208.066	539.7163	0.829904
10376	1215.473	539.531	0.824532
10377	1222.822	538.877	0.816025
10378	1230.375	538.668	0.861471
10379	1237.946	538.5037	0.883428
10380	1245.591	538.3931	0.935763
10381	1253.242	538.2411	0.715637
10382	1260.987	537.9691	0.715319
10383	1268.737	537.756	0.733229
10384	1277.136	537.5584	0.734879
10385	1284.982	537.3185	0.749112
10386	1293.252	536.9634	0.762781
10387	1301.583	536.6906	0.784112
10388	1309.994	536.5339	0.773006
10389	1318.541	536.3233	0.78813
10390	1327.149	536.0432	0.778944
10391	1335.649	535.6087	0.753025
10392	1344.576	535.377	0.736868
10393	1353.686	534.6899	0.749217
10394	1362.673	534.2408	0.765035
10395	1371.844	533.8262	0.788835
10396	1381.111	533.5316	0.796452
10397	1390.457	533.3218	0.811736
10398	1400.052	532.5729	0.860977
10399	1409.529	532.2603	0.895197
10400	1419.048	531.9167	0.929485
10401	1428.418	531.7455	0.708057
10402	1438.163	531.3766	0.721714
10403	1448.278	531.1038	0.716892
10404	1458.1	530.6785	0.720868
10405	1468.372	530.0702	0.73424
10406	1478.679	529.7255	0.726312
10407	1489.011	529.635	0.715685
10408	1499.881	528.9132	0.733461
10409	1510.319	528.4615	0.741212
10410	1521.028	528.1122	0.753755
10411	1531.749	528.008	0.754156
10412	1542.54	527.7783	0.748854

10413	1553.588	527.5043	0.72482
10414	1564.713	527.1692	0.714199
10415	1575.624	527.0143	0.737838
10416	1587.023	526.87	0.728866
10417	1599.35	526.2344	0.728073
10418	1611.311	526.0384	0.728732
10419	1623.226	525.7233	0.749189
10420	1634.948	525.2889	0.764204
10421	1647.357	525.1381	0.770551
10422	1659.862	524.5325	0.770319
10423	1672.513	524.3641	0.781215
10424	1685.613	524.2554	0.76523
10425	1698.172	523.8723	0.760992
10426	1711.424	523.6017	0.780216
10427	1724.745	523.1598	0.822223
10428	1738.133	522.8674	0.848139
10429	1751.414	522.5125	0.833409
10430	1765.273	522.2071	0.829704
10431	1779.345	521.5836	0.835856
10432	1793.844	520.9503	0.864019
10433	1808.229	520.2095	0.876879
10434	1823.144	519.9617	0.85963
10435	1837.872	519.2243	0.852104
10436	1853.111	518.3457	0.907391
10437	1868.132	517.858	1
10438	1883.474	517.3969	0.941475
10439	1899.372	516.5905	0.907632
10440	1916.156	515.6627	0.79978

The Engineering Meetings Board has approved this paper for publication. It has successfully completed SAE's peer review process under the supervision of the session organizer. The process requires a minimum of three (3) reviews by industry experts.

ISSN 0148-7191

http://papers.sae.org/2016-01-1478